

Production of a canine model of Parkinson's disease using somatic cell nuclear transfer

Ji Hye Lee

Chungnam National University

Kyu Kwon

Korea Advanced Institute of Science and Technology

Chan Kyu Park

Korea Advanced Institute of Science and Technology

Keun Jung Kim

Institute of Chungnam Livestock Research

Eun Young Kim

MK biotech

Min Kyu Kim (✉ kminkyu@cnu.ac.kr)

Chungnam National University

Article

Keywords: human DJ-1, somatic cell nuclear transfer, canine, depression

Posted Date: April 19th, 2022

DOI: <https://doi.org/10.21203/rs.3.rs-1543785/v1>

License:  This work is licensed under a Creative Commons Attribution 4.0 International License.

[Read Full License](#)

Abstract

Dogs have been considered a suitable model to study human neurodegenerative diseases, such as Alzheimer's disease and Parkinson's disease (PD), and brain aging, because of their long lifespan and the similarities of disease presentation and clinical response in humans and dogs. Further, it is possible to evaluate the visible cognition/motion ability of patients with brain dysfunction. In the present study, we aimed to generate a canine model of PD that overexpresses the human DJ-1 (hDJ-1) gene using the somatic cell nuclear transfer (SCNT) technique. The hDJ-1 gene was transfected into canine fetal fibroblasts, which were used to produce cloned embryos. Reconstructed embryos were transferred into the oviduct of surrogate mothers, one of which gave birth to one dog. The cloned dog was depressed, and his movements were slow and fewer, resulting in an abnormal phenotype, as observed via imaging analyses, such as positron emission tomography (PET) and magnetic resonance imaging (MRI) analyses; these findings were similar to the symptoms of PD in humans. In addition, exogenous hDJ-1 was successfully transmitted to the next generation without silencing. We confirmed that the puppies exhibited the same behavior and imaging analysis as the hDJ-1 transgenic (TG) dog. Using SCNT, we generated TG dogs with PD that overexpressed the hDJ-1 gene. Human PD-like phenotypes have been confirmed in the TG dogs. To the best of our knowledge, this is the first report that describes the establishment of a canine model of PD. Furthermore, TG dogs could be used in preclinical trials of drugs for the treatment of PD.

Introduction

Parkinson's disease (PD) is the most common neurodegenerative disease, affecting > 1% of the population over the age of 60 y. The neuropathology of PD includes the loss of dopaminergic neurons in the substantia nigra (SN), subsequent depletion of dopamine in the striatum, and the presence of Lewy bodies that are abnormal accumulations of α -synuclein¹. The motor symptoms of PD are bradykinesia, rest tremor, muscle rigidity, flexed posture, freezing of gait, and postural instability². Additionally, PD is accompanied by non-motor signs, such as depression, hallucinations, dementia, anxiety, autonomic insufficiency, sleep disorders, and emotional as well as cognitive deficits³. Even though the events leading to the degeneration of dopaminergic neurons in PD remains unknown, the interactions between genetic and environmental factors seem to be responsible for this. At present, there are no means of delaying or arresting the progression of PD; nevertheless, alleviation of symptoms is feasible with therapy.

Several genes, such as the ones encoding α -synuclein, parkin, protein deglycase DJ-1 (DJ-1) or Parkinson disease protein 7 (PARK7), ubiquitin carboxy-terminal hydrolase L1 (UCH-L1), cation-transporting ATPase 13A2 (ATP13A2), phosphatase and tensin homolog deleted on chromosome 10 (PTEN)-induced putative kinase 1 (PINK1), leucine-rich repeat kinase 2 (LRRK2), glucocerebrosidase 1 (GBA1), and vacuolar protein sorting 35 (VPS35), are reportedly associated with inherited forms of familial PD⁴⁻⁶. Moreover, *DJ-1* is an oncogene coding for a 189-amino acid-long protein, and it is associated with the early-onset,

autosomal, recessive form of PD^{7,8}. In fact, DJ-1 seems to have diverse roles; for instance, it is a regulatory subunit of the RNA-binding protein complex, it protects cells against oxidative stress, exhibits chaperone activity in an oxidized form, and subsequently inhibits the aggregation of α -synuclein⁹⁻¹¹. Recent studies suggest that although DJ-1 is not crucial for normal mitochondrial function, under certain conditions, like oxidative stress, it can prevent the degeneration and aggregation of oxidized mitochondrial proteins, thereby maintaining normal mitochondrial functions^{12,13}. Interestingly, Lee J. Y. et al. reported that human DJ-1 (hDJ-1), a glyoxalase, can protect cells and neurons from glyoxals in mice as well as in *Caenorhabditis elegans* and especially, preserve dopaminergic neurons¹⁴. Therefore, abnormalities in DJ-1 possibly contribute to neurodegeneration.

Reproducible animal models of PD are necessary for determining the cause of the disease, the mechanism of its progression, and for developing novel drugs and therapeutic methods. Initially, PD models were generated by administering neurotoxins and by genetic modification. In 1957, Carlsson A. et al. first reported the development of an animal model by inducing a deficiency of brain catecholamines using reserpine, which led to a temporary dopamine loss and akinesia¹⁵. In another study, 6-hydroxydopamine (6-OHDA) was directly injected into the rodent's striatum, leading to an immediate damage to the dopaminergic neurons in the medial forebrain bundle¹⁶. However, it has been reported that Lewy bodies are not deposited in these 6-OHDA models of PD¹⁷. Furthermore, upon administering 1-methyl-4-phenyl-1,2,3,6-tetrahydropyridine (MPTP) in Rhesus monkeys, they exhibited PD symptoms similar to those of humans as well as accumulation of Lewy bodies¹⁸. Although the MPTP animal models are ideal for studying PD, the protocol is not standardized, and hence, it is not applicable to mice. Incidentally, transgenic (TG) mice have been produced by insertion, deletion, and mutation of PD-associated genes. In fact, mice models with overexpression or A53T mutation of α -synuclein presented symptoms of early onset PD and Lewy body deposits in their brains¹⁹. Additionally, there are reports of knockout (KO) mice models of PINK1²⁰, parkin²¹ or DJ-1²². Even though these TG mouse models have exhibited the regression of dopaminergic neurons in the striatum, it is difficult to observe the complete development of PD due to their short lifespans.

Recently, Guangxi Bama minipigs with mutations in three PD-causing genes were generated using clustered regularly interspaced short palindromic repeats (CRISPR)/CRISPR-associated protein 9 (Cas9) and somatic cell nuclear transfer (SCNT), but α -synuclein pathology and loss of SN dopaminergic neurons were not detected²³. Moreover, KO pigs with the bi-allelic *DJ-1* gene were generated using a combination of transcription activator-like effector nucleases (TALENs) with SCNT²⁴. Although the efficiency of SCNT and gene editing in producing TG animals is still low, it is easier to execute than pronuclear injection or intracytoplasmic sperm injection (ICSI) for the production of animals with homologous recombination (HR) transgenes.

Dogs have a long lifespan and are easy to handle; moreover, it is possible to evaluate changes in their cognition and motion abilities owing to brain dysfunction. They naturally develop age-related neurodegenerative diseases such as Alzheimer's disease (AD) and PD. The most common symptoms of

PD in dogs include leg tremors, restlessness, stiff or inflexible muscles, and unusually cautious or slow movements. Similar to humans, there is no cure for these diseases in dogs, as well. In this study, we established *hDJ-1* transfected cells by viral infection and produced a TG dog overexpressing the *hDJ-1* gene using SCNT. The dog was evaluated by behavioral tests and brain imaging analysis, and it displayed PD-like symptoms.

Results

Establishment of *hDJ-1* overexpressing cell line

Canine fetal fibroblasts (CFFs) were transfected by a retroviral vector containing the *hDJ-1*, murine stem cell virus (MSCV) promoter, and puromycin resistance gene. A TG cell line was established (Fig. 1A), and the expression level of *hDJ-1* protein was confirmed by western blotting. Incidentally, the *hDJ-1* protein was detected in the TG cells, but not in the wild-type CFFs (Fig. 1B). After confirming the successful transfection of *hDJ-1* into the cells, these were used for SCNT.

Production of the *hDJ-1* TG dog

The *hDJ-1* overexpressing cells were used as donor cells to produce the TG dog. These cells were injected into 72 enucleated oocytes, of which 38 underwent successful fusion (52.8%). These 37 SCNT embryos were surgically transferred into the oviducts of 5 surrogate mothers (Table 1), out of which 1 (20%) was confirmed to be pregnant. This pregnant female was monitored by ultrasonography every 2 w (Fig. 2A), and she gave birth to a healthy puppy weighing 412 g by cesarean section (Fig. 2B), thereby confirming that gene editing of TG cells did not impair the cell reprogramming of cloned dogs. The SCNT efficiency was 2.6% (1/38).

Table 1
In vivo development of SCNT embryos overexpressing the *hDJ-1* gene

No. of SCNT oocytes	No. of fused embryos ¹	No. of transferred embryos	No. of recipients	No. of successful pregnancies ²	No. of cloned dogs ³
72	38 (52.8%)	38	5	1 (20%)	1 (2.6%)

¹Percentage is calculated based on the number of SCNT-derived oocytes. ²Percentage is calculated based on the number of recipients. ³Percentage is calculated from the number of transferred embryos. *hDJ-1* – human protein deglycase DJ-1 gene; SCNT – somatic cell nuclear transfer

Characterization of the *hDJ-1* TG dog

We assessed the *hDJ-1* protein levels in the blood of the TG dog as well as the controls using western blotting. Interestingly, the *hDJ-1* protein was strongly expressed in the blood of the TG dog, whereas the

control dogs did not express it at all (Fig. 3A). To confirm the *hDJ-1* insertion site and its copy number in the chromosome of the TG dog, inverse polymerase chain reaction (PCR) was performed. First, the *hDJ-1* (3–4 kb) was detected using primary PCR, and this PCR product was used for the secondary PCR. Consequently, a gene fragment that was 1–2 kb in size was detected in the TG dog (Fig. 3B). The sequencing results indicate that five *hDJ-1* genes have been inserted into chromosomes 2 (55,177,097), 9 (50,670,666), 11 (67,945,360 and 69,841,723), and 26 (35,481,313) of the TG dog.

The *hDJ-1* TG dog displays a PD-like phenotype

After 7 m of birth, the *hDJ-1* TG dog repeatedly displayed symptoms of depression that continued for 5–10 d until the onset of puberty. At this point, he exhibited a flexed posture (Fig. 4A) and experienced tremors, stiffness, and decreased stability. Moreover, he did not jump and eat, moved slowly, and faced difficulty in getting up from a lying posture (supplementary video S1). In the knuckling test, when the dog’s paw was flipped, it did not return to the original position (Fig. 4B). Additionally, in the 10 m running test, the control dogs covered the distance in 3 s, while the TG dog walked slowly and reached the finish line after 17 s (Table 2, supplementary video S2, and S3). The puberty onset of the *hDJ-1* TG dog was late, and the sex organ development, including penis and testis, was slow, as compared to that of the control dogs.

Table 2
Comparison of running times of control and transgenic dogs during 10 m running test

	Time (s)
Control	3
<i>hDJ-1</i> TG dog	17
This experiment was repeated three times independently. <i>hDJ-1</i> TG – human protein deglycase DJ-1 gene overexpressed transgenic.	

Germ line transmission of *hDJ-1* in the TG dog

When the *hDJ-1* TG dog reached puberty, semen sample was collected and artificially inseminated into the oviducts of wild-type female beagles. Ultimately, 6 females delivered 28 pups (Fig. 5A), but 12 of them died after birth due to an unknown cause. The presence of *hDJ-1* in all the pups was confirmed by PCR. Additionally, the insertion site of *hDJ-1* was identified by inverse PCR (Table 3). Incidentally, six pups displayed similar behavior to that of the *hDJ-1* TG dog. For 5-10 d, they suffered from depression, flexed posture, and tremors, walked slowly, and experienced pain when people touched them. They could not straighten their toes (Fig. 5), and when people called out to them, they struggled to get up, but could not (supplementary video S4). Furthermore, in the 10 m running test, while the control dogs covered the distance in 4.8 s, the depressed offspring walked slowly and reached the finish line in 22 s.

Table 3

Confirmation of germline transmission of *hDJ-1* based on analyses of offspring of *hDJ-1* transgenic dog

Offspring No.	Insertion of <i>hDJ-1</i>					Sex ¹	Phenotype ²
	chr. 2	chr. 9	chr. 11 - 1	chr. 11 - 2	chr. 26		
O 1-1		+	+			M	O
O 1-2	+			+	+	M	
O 2-1				+	+	M	
O 2-2	+	+		+	+	F	
O 2-3	+					F	
O 2-4			+			M	
O 3-1		+	+			M	
O 3-2				+	+	F	
O 3-3	+		+	+	+	M	
O 3-4		+	+		+	M	
O 3-5		+	+			M	O
O 3-6	+			+	+	M	
O 3-7	+		+			M	O
O 3-8	+	+		+	+	M	
O 4-1			+		+	F	O
O 4-2	+			+	+	M	
O 4-3	+			+	+	M	
O 4-4	+	+	+		+	M	
O 4-5		+		+	+	M	O
O 5-1				+	+	M	
O 5-2	+			+	+	M	
O 5-3	+		+			F	
O 6-1	+	+	+		+	F	
O 6-2				+	+	M	

¹ F, female; M, male. ² Phenotype "O" indicates depression, slow behavior, and muscle stiffness. *hDJ-1* – human protein deglycase DJ-1 gene; chr. – chromosome.

Offspring No.	Insertion of <i>hDJ-1</i>					Sex ¹	Phenotype ²
	chr. 2	chr. 9	chr. 11 - 1	chr. 11 - 2	chr. 26		
O 6 - 3	+	+		+	+	F	O
O 6 - 4			+			M	
O 6 - 5		+		+	+	M	
O 6 - 6	+		+		+	F	

¹ F, female; M, male. ² Phenotype "O" indicates depression, slow behavior, and muscle stiffness. *hDJ-1* – human protein deglycase DJ-1 gene; chr. – chromosome.

Imaging analysis of the hDJ-1 TG dog

The brains of 3-y-old *hDJ-1* TG dog and 2-y-old control dog were subjected to imaging analyses, such as magnetic resonance imaging (MRI) and positron emission tomography-computerized tomography (PET-CT) imaging analyses. As shown in Fig. 6, the *hDJ-1* TG dog exhibited significant loss of striatal dopamine transporter (DAT) binding and enlargement of both cerebral ventricles, as compared to that in the control. The binding potential (BP) value of the *hDJ-1* TG dog was 4.53, resulting in a 2-fold reduction in the striatal N-(3-[¹⁸F]fluoropropyl)-2 β -carboxymethoxy-3 β -(4-iodophenyl) nortropine ([¹⁸F]-FP-CIT) uptake, as compared to that of the control (8.09).

Discussion

Majority of the animal models for PD include small animals, such as mice and rats. These rodent PD models were developed by neurotoxin treatment, such as 6-OHDA and MPTP, and by KO or mutation of PD-related genes. Incidentally, these rodent PD models have reported a severe degeneration of nigral neurons and a decrease in dopamine secretion. Many such small animal models of PD exhibit PD-like symptoms, but they are insufficient for studying the disease due to their short lifespans. Previously, dogs injected with MPTP have displayed severe PD-like motor symptoms, including bradykinesia, head tremor, and postural instability²⁵. In this study, *hDJ-1* was used to generate cloned dogs as a PD animal model. For this, SCNT was performed to produce reconstructed embryos with CFFs expressing *hDJ-1*, and the fused embryos were transferred into the oviducts of recipients. One dog was born from one of the surrogates, and the hDJ-1 protein was expressed in the blood of this dog. Therefore, it was confirmed that the cloned dog is a TG dog expressing the exogenous hDJ-1 protein generated by SCNT.

In humans, typical PD symptoms include resting tremor, akinesia, muscle rigidity, postural instability, autonomic insufficiency, cognitive impairment, and sleep disorders. Additionally, depression is a common disorder in these patients, often leading to a reduced quality of life²⁶. After 7 m of birth, the cloned dog exhibited first symptoms of depression. Similar to humans, the depressed dog did not eat, and his movements were slow and restricted. Furthermore, behavior analyses of the *hDJ-1* TG dog indicated flexed posture, tremor, slow walking, and decreased stability, similar to the PD symptoms of humans.

Neurological examination revealed that the *hDJ-1* TG dog experienced difficulty in returning his paw to the original position after being flipped. This suggested neurological deficits in the dog. A previous study had reported that MPTP-treated canines exhibited rigidity, severe akinesia, and anergia in response to peripheral sensory stimuli. Those dogs stood with splayed legs, stayed in that position, stopped eating, and lost balance during movement²⁵. The behavior of the *hDJ-1* TG dog of this study was similar to that of the MPTP-treated canines. These results indicate that the TG dog displayed PD-like motor symptoms.

It is possible that the expression of exogenous genes in TG animals is affected by epigenetic modifications during transmission to the next generation, resulting in the suppression of transgene expression by silencing²⁷. To test whether *hDJ-1* can be transmitted to the next generation, sperm samples of the *hDJ-1* TG dog were collected and artificially inseminated into wild-type female dogs. This study reported that all the puppies born to these surgically inseminated females exhibited confirmed integration of *hDJ-1* in their chromosomes, and the insertion sites were identical to those in the *hDJ-1* TG dog. Therefore, exogenous *hDJ-1* was successfully transferred to the offspring of the next generation without undergoing silencing.

Imaging analyses, such as PET-CT and MRI, were performed in the TG dog to diagnose PD pathology that is visible as structural and functional abnormalities in the brain. The *hDJ-1* TG dog has an abnormal phenotype regarding the size of the ventricles, unlike control dogs, which have no difference between the sizes of the two ventricles. Moreover, PET-CT detected asymmetrically decreased FP-CIT uptake in the striatum of the *hDJ-1* TG dog; specifically, the right and left sides of the striatum were different, unlike that of the control dogs. This result suggested abnormality in dopamine secretion, and the imaging results of the *hDJ-1* TG dog were similar to that of human PD patients.

In conclusion, we have generated the first canine PD model using the SCNT technique. Reconstructed embryos derived from *hDJ-1* overexpressing cells were used to successfully induce pregnancy in the recipient mother, and the *hDJ-1* gene of the TG dogs was transmitted through the germ line to the next generation. The brain imaging and behavior of the *hDJ-1* TG dog were similar to that of human PD patients. Future investigations are needed to identify α -synuclein-immunopositive pathology or loss of SN dopaminergic neurons in dogs with *hDJ-1* TG. Animal models are essential in the field of PD research, the *hDJ-1* TG dogs will be used in clinical trials, which will significantly contribute to drug development.

Methods

Chemicals

All chemicals were purchased from Sigma-Aldrich (St. Louis, MO, USA), unless otherwise stated.

Animal Ethics

The all experiments were approved by the Institutional Animal Care and Use Committee (IACUC) of Chungnam National University (Approval No. : CNU-00012) and performed according to “The Guidelines for the Care and Use of Laboratory Animals” published by the IACUC of Chungnam National University. And this study was carried out in compliance with the ARRIVE guidelines. 14 female mongrel dogs between 2 and 6 years of age (body weight: 25–35 kg) were used as oocyte donors and surrogate mothers, and purchased from Honghwa Inc. (Nonsan, Korea). And 6 beagles from 2 to 6 years of age (body weight: 8–10 kg) purchased from ORIENT BIO Inc. (Seongnam, Korea) were used in this study for breeding. Dogs were raised indoors in separate cages with a 22–23°C temperature, 50–60% humidity and ventilation control system. They were fed commercial diet once daily and provided water *ad libitum*. They fed commercial diet (GOOD BOY JINDO, JEILpetfood, Seoul, Korea) at twice a day (09:00, 17:00), and freshwater was provided freely.

Construction of retroviral vector containing hDJ-1 and establishment of transgenic cell line

The gene sequence encoding the hDJ-1 protein was obtained from the human cDNA library. For N-terminal FLAG tagging, the *hDJ-1* was cloned into pcDNA3.1(+)_Flag using *hDJ-1_Hind III*_forward (F) (5'-GGAAGCTTATGGCTTCCAAAAGAGCTCT-3') and *hDJ-1_Xho I*_reverse (R) (5'-GGGCTCGAGCTAGTCTTTAAGAACAAGTG-3') primers. The retroviral plasmid MSCV (pMSCV)-puro vector, which includes the MSCV promoter, long terminal repeat (LTR), virus packaging signal (Ψ +), and puromycin resistance gene, was used for *hDJ-1* transfer (Fig. 7). After PCR amplification of *hDJ-1*, it was inserted into the pMSCV-puro vector using FLAG_*Xho I*_F (5'-CCCCTCGAGATGGACTACAAAGACGAT-3') and *hDJ-1_EcoRI*_R (5'-GGGAATTCCTAGTCTTTAAGAACAAGTG-3') primers.

The 293T cell line, which is derivative of human embryonic kidney 293 cells, were used as retrovirus-packaging cells, and polyethyleneimine (PEI) was used to transfect the cells with the FLAG-tagged *hDJ-1* in the pMSCV vector. The retroviral vector-containing medium was harvested after 48 h of transfection. Thereafter, 10^6 CFFs/mL were seeded on a 100 mm dish (Falcon®, CORNING INC., Arizona, USA) and transfected with the retroviral vector in the presence of 6 μ g/mL polybrene. The transfected cells were selected using puromycin. Finally, the live cells were isolated, proliferated, and stored at -196°C until further use.

Collection of in vivo matured oocytes

Blood was collected every day from 14 dogs on the first day of estrus, and serum progesterone (P4) concentrations were measured using a DSL-3900ACTIVE progesterone coated-tube radioimmunoassay kit (Diagnostic Systems Laboratories, Inc., TX, USA). The day when P4 concentration reached 4.0–7.0 ng/mL was considered as the day of ovulation. *In vivo* matured oocytes were collected by laparotomy after 3 d of ovulation. The dogs were anesthetized using 6 mg/kg ketamine and xylazine, and the anesthesia was maintained with 2% isoflurane. The ovaries and uterus were exteriorized by an aseptic surgical procedure. For oviductal flushing, an inverted flanged bulb steel needle (18-gauge, 7.5 cm) was inserted through the bursal slit and held in position using a plastic tube and hemostatic forcep.

Subsequently, a 24-gauge intravenous (IV) catheter (Angiocath™ Plus, Becton Dickinson Korea Inc., Seoul, Korea) was inserted into the oviductal lumen near the uterotubal junction. Approximately 10 mL of media 199 (Gibco™, Thermo Fisher Scientific Inc., Massachusetts, USA) supplemented with 10 mM HEPES, 2 mM NaHCO₃, 0.013 mM kanamycin, and 0.5% bovine serum albumin (BSA; Gibco™) was injected through the IV catheter into the oviduct. The 93 ovulated oocytes were flushed out via the steel needle and immediately transported to the laboratory.

SCNT And Embryo Transfer

The SCNT was performed according to a previously described protocol^{28,29}. First, the cumulus cells were removed from the *in vivo*-matured oocytes using 0.1% hyaluronidase. Thereafter, the first polar body and nucleus were removed in HEPES-buffered media 199 containing 5 µg/mL Hoechst 33342 and 5 µg/mL cytochalasin B using manipulators under an inverted microscope equipped with epifluorescence. Subsequently, a TG cell was injected into the perivitelline space of the enucleated oocyte. The couplets were electrically fused by two pulses of direct current (70–73 V for 15 µs) into a 0.26 M mannitol fusion medium containing 0.1 mM HEPES, 0.5 mM MgSO₄, and 0.05% BSA using an Electro-Cell Fusion apparatus (NEPA Gene Co., Chiba, Japan). After incubation for 1 h 30 min in porcine zygote medium-3 (PZM-3), the embryos were examined. The fused embryos were chemically activated in 10 µM calcium ionophore for 4 min, washed in PZM, and incubated in 1.9 mM 6-dimethylaminopurine (6-DMAP) for 3 h 30 min. Within 4 h of SCNT, the reconstructed embryos were transferred into the oviducts of naturally synchronized surrogate mother dogs using laparotomy. The cloned embryos were placed in the uterotubal junctions of the oviducts using an Argyle™ sterile tom-cat catheter (Medtronic Inc., Minnesota, USA). Pregnancy was confirmed using a MyLab30vetGold (Esaote, Genoa, Italy) ultrasound scanner with a variable-band convex array probe 25 to 30 d after embryo transfer.

Western Blotting

For western blot analysis, the CFFs, *hDJ-1* transfected cells, and blood collected from control dogs as well as the *hDJ-1* TG dog were lysed in radioimmunoprecipitation assay buffer [20 mM Tris-HCl, pH 7.5; 100 mM NaCl; 1 mM ethylenediamine tetracetic acid (EDTA); 2 mM ethylene glycol-bis(β-aminoethyl ether)-N,N,N',N'-tetraacetic acid (EGTA); 1 mM Na₃VO₄; 50 mM β-glycerophosphate; 50 mM NaF; 1% Triton X-100; and protease inhibitor cocktail]. The cell lysates were separated by sodium dodecyl sulfate (SDS)-polyacrylamide gel electrophoresis (PAGE) and transferred to a nitrocellulose membrane. The nitrocellulose membranes were blocked for 2 h in 5% skim milk and incubated overnight at 4°C with anti-actin and anti-PARK7/DJ-1 (Abcam®, Cambridge, UK) antibodies. Thereafter, the membranes were washed three times and incubated with horseradish peroxidase-conjugated secondary antibodies. Finally, the membranes were developed, and the hDJ-1 proteins were visualized using LAS-4000 (Fujifilm Life Sciences, Massachusetts, USA).

Behavioral Tests Of The Tg Dog

When the TG dog appeared depressed, he was subjected to the knuckling test and 10 m walking test. The knuckling test, which determines the time taken by the dog to return his paw to the normal position after being flipped, is used to check the nerve reflex of the dog. In the 10 m walking test, the TG dog and control dogs were placed at a starting line. The tester, who was 10 m away from the starting line, enticed dogs to run, and the scorer recorded the time taken by each dog to reach the finish line.

Inverse Pcr

Genomic DNA of TG dogs was digested using *BamHI* and self-ligated using T4 ligase. Subsequently, PCR was conducted according to the following conditions: 95°C for 5 min; 35 cycles of 95°C for 30 s, 61.4°C for 40 s, and 72°C for 6 min; and a final extension at 72°C for 10 min. The first PCR was performed using IN_ *hDJ-1*_F (5'-CTGAGAATCGTGTGGAAAAAGACGGCC-3') and IN_ *hDJ-1*_R (5'-GATGACCAGTCTTTTGAAGCCAT-3') primers. The second PCR was performed using the PCR products of the first PCR. For this, IN_ *hDJ-1*_F (5'-CTGAGAATCGTGTGGAAAAAGACGGCC-3') and IN_LTR_R (5'-GCCCATATTCTGCTGTCTCTGTTCC-3') primers were used, and the insertion sites of *hDJ-1* were identified by sequencing.

Surgical Insemination Of Dogs

To confirm the germ-line transmission of *hDJ-1*, the TG dog was artificially bred with wild-type female dogs via surgical insemination. Semen was collected from the TG dog and washed with phosphate buffered saline (PBS; Gibco™). The sperms were diluted with 1 mL PBS and stored at 37°C until artificial insemination (AI) was performed on the bitches via laparotomy. After 2 d of ovulation, the uteri of the 5 female dogs were exposed through abdominal incisions. Sperm samples were injected into the uterine horn using a 3 mL syringe and a 24-gauge IV catheter. Approximately 28 d after AI, pregnancy was confirmed using ultrasound imaging, and after 60 d of AI, the offspring of *hDJ-1* TG dog were born via vaginal delivery.

In vivo MRI

The *hDJ-1* TG dog and one wild-type control dog were subjected *in vivo* MRI of the brain to evaluate the structural changes. The TG dog was 3-y-old and control dog was 2-y-old, and weighed 9–10 kg. They were fasted for at least 20 h prior to the scan. Before conducting the MRI, each dog was anesthetized with ketamine (6 mg/kg, IV). Subsequently, the dog was transferred to the MRI table and immobilized in the prone position. The anesthesia was maintained with 2% isoflurane in 99.9% oxygen (2 L/min) throughout the procedure. Pulse rate and body temperature of the dogs were monitored continuously, and the body temperature was maintained with a warm blanket surrounding the animal. All MRI experiments were performed using a Philips 3T Achieva scanner (Philips Medical System, Best, Netherlands) with a

32-channel head coil at the Korea National Primate Center³⁰. The MRI included whole-head T1-weighted and T2-weighted images. The T1-weighted imaging was performed with a three-dimensional (3D) turbo field echo (TFE) sequence with the following parameters: repetition time (TR) = 14 ms, echo time (TE) = 6.8 ms, field of view (FOV) = 13 × 13 cm, 150 slices, slice thickness = 0.5 mm, acquisition matrix size = 260 × 165, voxel size = 0.5 × 0.79 × 0.5 mm, 4 number of signals averaged (NSA). The 3D T2-weighted imaging was performed with a 3D turbo spin echo (TSE) sequence with the following parameters: TR = 2,500 ms, TE = 217 ms, FOV = 13 × 13 cm, 150 slices, slice thickness = 0.5 mm, acquisition matrix size = 260 × 260, voxel size = 0.5 × 0.5 × 0.5 mm, 1 NSA.

In vivo PET-CT imaging

All *in vivo* PET images were acquired using a PET-CT scanner (Biograph-mCT s20-3R; Siemens Medical Systems, Knoxville, USA). After the MRI, the dogs were transferred to the PET-CT table and immobilized in the prone position. The anesthesia was maintained with 2% sevoflurane in 99.9% oxygen (2 L/min). The [¹⁸F]-FP-CIT (DuChemBio Co., Ltd., Daejeon, Korea) PET imaging was performed to detect the dopamine transporters³¹. The dogs were administered 5 mCi of [¹⁸F]-FP-CIT intravenously, followed by CT scan for attenuation correction. Scanning began at the same time as radiotracer injection. The brain PET images of 400 × 400 matrix size were acquired by a 39-frame dynamic sequence for 120 min, according to the following pattern: 15 sec × 8, 30 sec × 6, 60 sec × 5, 120 sec × 5, 300 sec × 10, and 600 sec × 5. The images were reconstructed using a standard iterative algorithm (OSEM 3D + TOF) and post-processed using Syngo VG51C software (Siemens Medical Solutions, Erlangen, Germany) to visualize multiplanar fusion images.

Pet/mri Fusion Imaging And Quantitative Analysis

To fuse the images obtained during PET and MRI, the MRI data were processed using the software supplied by the manufacturer and converted to the DICOM format for co-registration with PET images. The PET and MR images were co-registered on IRW software (Inveon Research Workplace, Siemens Medical Solutions, USA) by rigid and manual registration³². The striatal binding potential was calculated by Logan's non-invasive graphical method using a reference region³³. The striatum was segmented by threshold-based automatic delineation of volume of interest (VOI) with the aid of MRI. The VOI of the cerebellum was selected as the reference region.

Statistical analysis

For each experiment there were at least 3 replicates, and data were analyzed using SPSS statistics 24 software (IBM SPSS statistics, Chicago, IL, USA).

Declarations

- **Ethics approval and consent to participate**

The entire study design was approved by the Institutional Animal Care and Use Committee (IACUC) of Chungnam National University (Approval No.: CNU-00012) and performed according to “The Guide for the Care and Use of Laboratory Animals” published by the IACUC of Chungnam National University.

- **Consent for publication**

Not applicable

- **Availability of data and materials**

Upon reasonable request, the datasets of this study can be available from the corresponding author.

- **Competing interests**

The authors declared no competing interests.

- **Funding**

This research was supported by a grant of the Korea Health Technology R&D Project through the Korea Health Industry Development Institute (KHIDI), funded by the Ministry of Health & Welfare, Republic of Korea (grant number : HI18C0660).

- **Acknowledgements**

We would like to thank Editage ([www. editage.co.kr](http://www.editage.co.kr)) for English language editing.

- **Authors' information**

Affiliations

Division of Animal and Dairy Science, College of Agriculture and Life Science, Chungnam National University, Daejeon, 34134, Republic of Korea

Ji Hye Lee and Min Kyu Kim

Department of Biological Sciences, Korea Advanced Institute of Science and Technology, Daejeon 34141, Republic of Korea

Kyu Kwon and Chan Kyu Park

Institute of Chungnam Livestock Research, Cheongyang 33350, Republic of Korea

Keun Jung Kim

MK biotech, 34134 Daejeon, Republic of Korea

- **Authors' contributions**

Conceptualization: J.H.L., K.K., C.K.P., M.K.K.; methodology, formal analysis, and investigation: J.H.L., K.K., K.K.K., E.Y.K.; resources: M.K.K.; original draft preparation: J.H.L.; review and editing: J.H.L., K.K., K.K.K., E.Y.K.; supervision and project administration: C.K.P.; research ethics and software: J.H.L., K.K., K.K.K., E.Y.K., M.K.K., funding acquisition: M.K.K. All authors have read and agreed to the published version of the manuscript

References

1. Forno, L. S. Neuropathology of Parkinson's disease. *J Neuropathol Exp Neurol* **55**, 259–272, doi:10.1097/00005072-199603000-00001 (1996).
2. Marsden, C. D. Parkinson's disease. *J Neurol Neurosurg Psychiatry* **57**, 672–681, doi:10.1136/jnnp.57.6.672 (1994).
3. Pont-Sunyer, C. *et al.* The onset of nonmotor symptoms in Parkinson's disease (the ONSET PD study). *Mov Disord* **30**, 229–237, doi:10.1002/mds.26077 (2015).
4. Zeng, X. S., Geng, W. S., Jia, J. J., Chen, L. & Zhang, P. P. Cellular and Molecular Basis of Neurodegeneration in Parkinson Disease. *Front Aging Neurosci* **10**, 109, doi:10.3389/fnagi.2018.00109 (2018).
5. Lubbe, S. & Morris, H. R. Recent advances in Parkinson's disease genetics. *J Neurol* **261**, 259–266, doi:10.1007/s00415-013-7003-2 (2014).
6. Maiti, P., Manna, J. & Dunbar, G. L. Current understanding of the molecular mechanisms in Parkinson's disease: Targets for potential treatments. *Transl Neurodegener* **6**, 28, doi:10.1186/s40035-017-0099-z (2017).
7. Bonifati, V. *et al.* Mutations in the DJ-1 gene associated with autosomal recessive early-onset parkinsonism. *Science* **299**, 256–259, doi:10.1126/science.1077209 (2003).
8. Nagakubo, D. *et al.* DJ-1, a novel oncogene which transforms mouse NIH3T3 cells in cooperation with ras. *Biochem Biophys Res Commun* **231**, 509–513, doi:10.1006/bbrc.1997.6132 (1997).
9. Shendelman, S., Jonason, A., Martinat, C., Leete, T. & Abeliovich, A. DJ-1 is a redox-dependent molecular chaperone that inhibits alpha-synuclein aggregate formation. *PLoS Biol* **2**, e362, doi:10.1371/journal.pbio.0020362 (2004).
10. Zhou, W. & Freed, C. R. DJ-1 up-regulates glutathione synthesis during oxidative stress and inhibits A53T alpha-synuclein toxicity. *J Biol Chem* **280**, 43150–43158, doi:10.1074/jbc.M507124200 (2005).
11. Zhou, W., Zhu, M., Wilson, M. A., Petsko, G. A. & Fink, A. L. The oxidation state of DJ-1 regulates its chaperone activity toward alpha-synuclein. *J Mol Biol* **356**, 1036–1048, doi:10.1016/j.jmb.2005.12.030 (2006).

12. Dodson, M. W. & Guo, M. Pink1, Parkin, DJ-1 and mitochondrial dysfunction in Parkinson's disease. *Curr Opin Neurobiol* **17**, 331–337, doi:10.1016/j.conb.2007.04.010 (2007).
13. Paterna, J. C., Leng, A., Weber, E., Feldon, J. & Büeler, H. DJ-1 and Parkin modulate dopamine-dependent behavior and inhibit MPTP-induced nigral dopamine neuron loss in mice. *Mol Ther* **15**, 698–704, doi:10.1038/sj.mt.6300067 (2007).
14. Lee, J. Y. *et al.* Human DJ-1 and its homologs are novel glyoxalases. *Hum Mol Genet* **21**, 3215–3225, doi:10.1093/hmg/ddc155 (2012).
15. Carlsson, A., Lindqvist, M., Magnusson, T. & Waldeck, B. On the presence of 3-hydroxytyramine in brain. *Science* **127**, 471, doi:10.1126/science.127.3296.471 (1958).
16. Thiele, S. L., Warre, R. & Nash, J. E. Development of a unilaterally-lesioned 6-OHDA mouse model of Parkinson's disease. *J Vis Exp*, doi:10.3791/3234 (2012).
17. Lindgren, H. S., Lelos, M. J. & Dunnett, S. B. Do α -synuclein vector injections provide a better model of Parkinson's disease than the classic 6-hydroxydopamine model? *Exp Neurol* **237**, 36–42, doi:10.1016/j.expneurol.2012.05.022 (2012).
18. Burns, R. S. *et al.* A primate model of parkinsonism: selective destruction of dopaminergic neurons in the pars compacta of the substantia nigra by N-methyl-4-phenyl-1,2,3,6-tetrahydropyridine. *Proc Natl Acad Sci U S A* **80**, 4546–4550, doi:10.1073/pnas.80.14.4546 (1983).
19. Lam, H. A. *et al.* Elevated tonic extracellular dopamine concentration and altered dopamine modulation of synaptic activity precede dopamine loss in the striatum of mice overexpressing human α -synuclein. *J Neurosci Res* **89**, 1091–1102, doi:10.1002/jnr.22611 (2011).
20. Cai, X. *et al.* In search of early neuroradiological biomarkers for Parkinson's Disease: Alterations in resting state functional connectivity and gray matter microarchitecture in PINK1 $-/-$ rats. *Brain Res* **1706**, 58–67, doi:10.1016/j.brainres.2018.10.033 (2019).
21. Pinto, M., Nissanka, N. & Moraes, C. T. Lack of Parkin Anticipates the Phenotype and Affects Mitochondrial Morphology and mtDNA Levels in a Mouse Model of Parkinson's Disease. *J Neurosci* **38**, 1042–1053, doi:10.1523/jneurosci.1384-17.2017 (2018).
22. Giangrosso, D. M., Furlong, T. M. & Keefe, K. A. Characterization of striatum-mediated behavior and neurochemistry in the DJ-1 knock-out rat model of Parkinson's disease. *Neurobiol Dis* **134**, 104673, doi:10.1016/j.nbd.2019.104673 (2020).
23. Zhu, X. X., Zhong, Y. Z., Ge, Y. W., Lu, K. H. & Lu, S. S. CRISPR/Cas9-Mediated Generation of Guangxi Bama Minipigs Harboring Three Mutations in α -Synuclein Causing Parkinson's Disease. *Sci Rep* **8**, 12420, doi:10.1038/s41598-018-30436-3 (2018).
24. Yao, J. *et al.* Efficient bi-allelic gene knockout and site-specific knock-in mediated by TALENs in pigs. *Scientific Reports* **4**, 6926, doi:10.1038/srep06926 (2014).
25. Choi, C. B. *et al.* Assessment of metabolic changes in the striatum of a MPTP-intoxicated canine model: in vivo ^1H -MRS study of an animal model for Parkinson's disease. *Magn Reson Imaging* **29**, 32–39, doi:10.1016/j.mri.2010.03.043 (2011).

26. Berghauzen-Maciejewska, K. *et al.* Pramipexole but not imipramine or fluoxetine reverses the "depressive-like" behaviour in a rat model of preclinical stages of Parkinson's disease. *Behav Brain Res* **271**, 343–353, doi:10.1016/j.bbr.2014.06.029 (2014).
27. Bordignon, V. *et al.* Transgene expression of green fluorescent protein and germ line transmission in cloned calves derived from in vitro-transfected somatic cells. *Biol Reprod* **68**, 2013–2023, doi:10.1095/biolreprod.102.010066 (2003).
28. Lee, B. C. *et al.* Dogs cloned from adult somatic cells. *Nature* **436**, 641–641, doi:10.1038/436641a (2005).
29. Lee, J. H. *et al.* Effect of acteoside as a cell protector to produce a cloned dog. *Plos one* **11**, e0159330 (2016).
30. Yeo, H.-G. *et al.* Characterization of cerebral damage in a monkey model of Alzheimer's disease induced by intracerebroventricular injection of streptozotocin. *Journal of Alzheimer's Disease* **46**, 989–1005 (2015).
31. Kazumata, K. *et al.* Dopamine transporter imaging with fluorine-18-FPCIT and PET. *Journal of Nuclear Medicine* **39**, 1521–1530 (1998).
32. Kim, S.-m. *et al.* Hybrid PET/MR imaging of tumors using an oleanolic acid-conjugated nanoparticle. *Biomaterials* **34**, 8114–8121 (2013).
33. Logan, J. *et al.* Distribution volume ratios without blood sampling from graphical analysis of PET data. *Journal of Cerebral Blood Flow & Metabolism* **16**, 834–840 (1996).

Figures

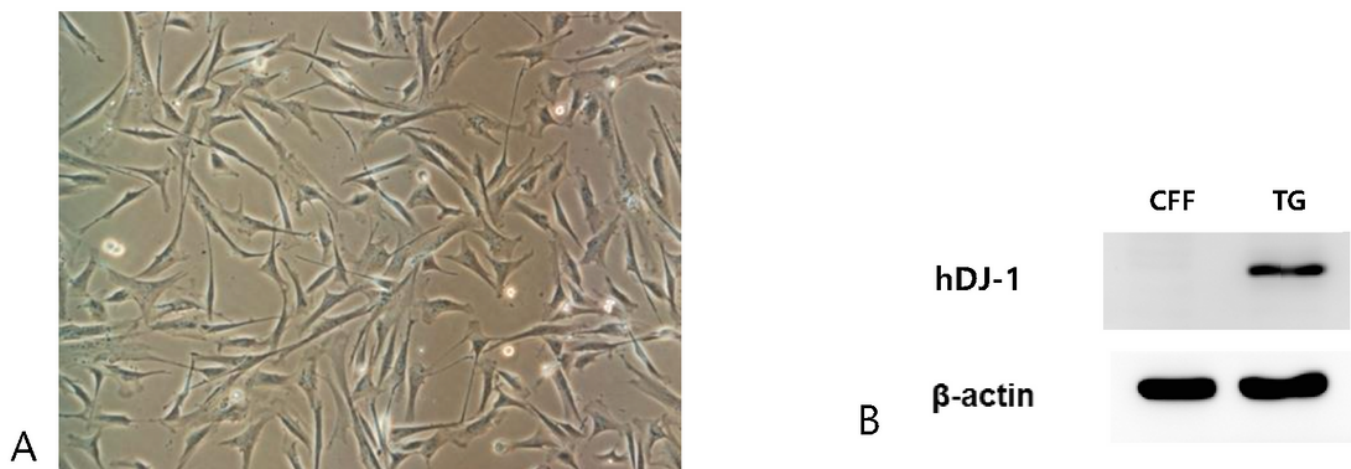


Figure 1

Generation of human protein deglycase DJ-1 (hDJ-1)-overexpressing canine fetal fibroblasts. **(A)** Morphology and **(B)** hDJ-1 protein expression of transgenic cells. CFF, canine fetal fibroblast; TG,

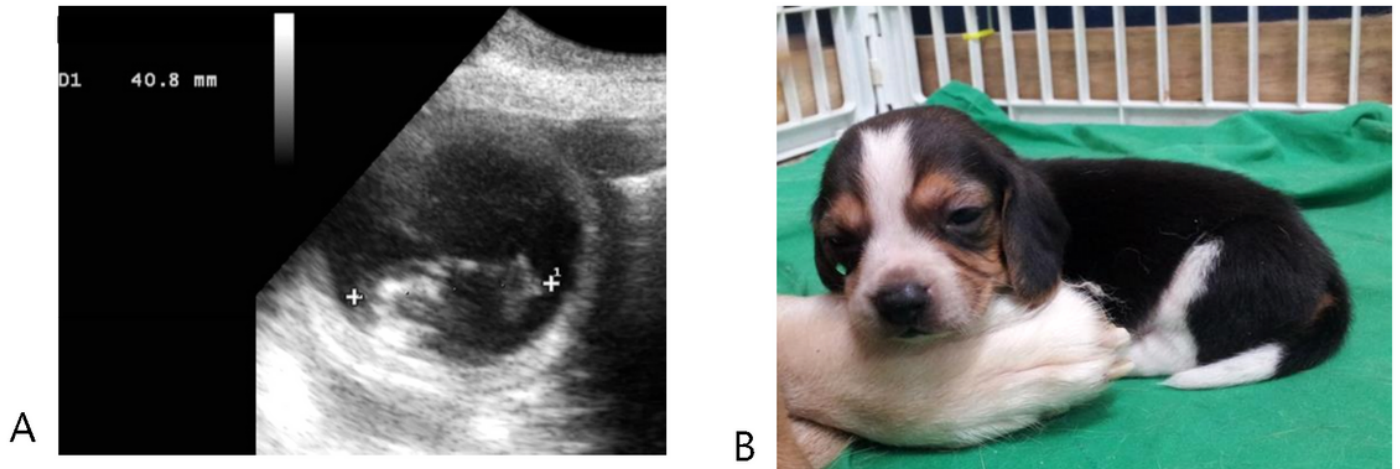


Figure 2

A transgenic dog. (A) Pregnancy confirmation by ultrasonography 40 d after embryo transfer. The size of fetus in the g-sac is 4 cm. (B) The 3-w-old cloned beagle.

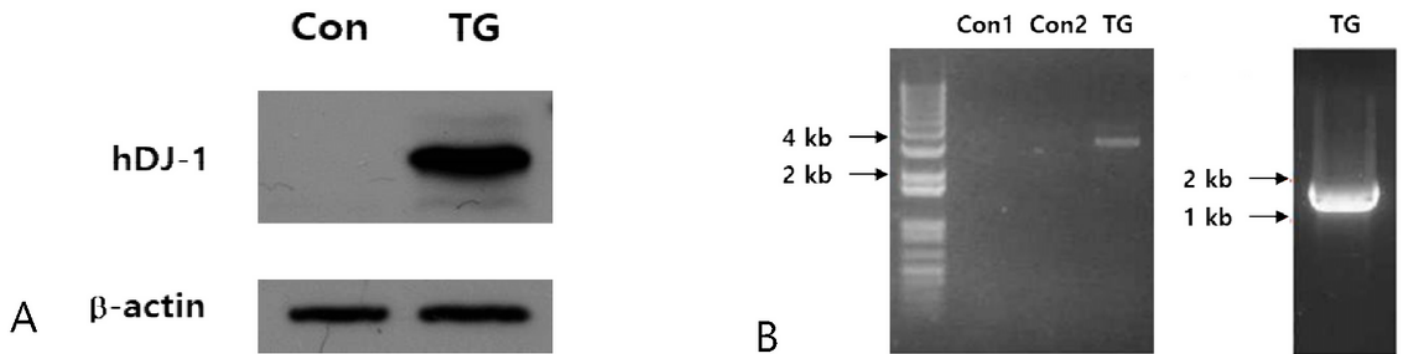


Figure 3

Genetic analysis of human protein deglycase DJ-1 gene (*hDJ-1*) from the transgenic dog. (A) Expression of hDJ-1 protein as detected by western blotting. (B) *hDJ-1_EcoRI* fragment amplification using inverse polymerase chain reaction (PCR) analysis. First PCR using IN_ *hDJ-1*_forward (F) and IN_ *hDJ-1*_reverse (R) primers and second PCR using IN_ *hDJ-1*_F and IN_ *hDJ-1*_R primers. Con, control dog; TG, *hDJ-1* transgenic dog.

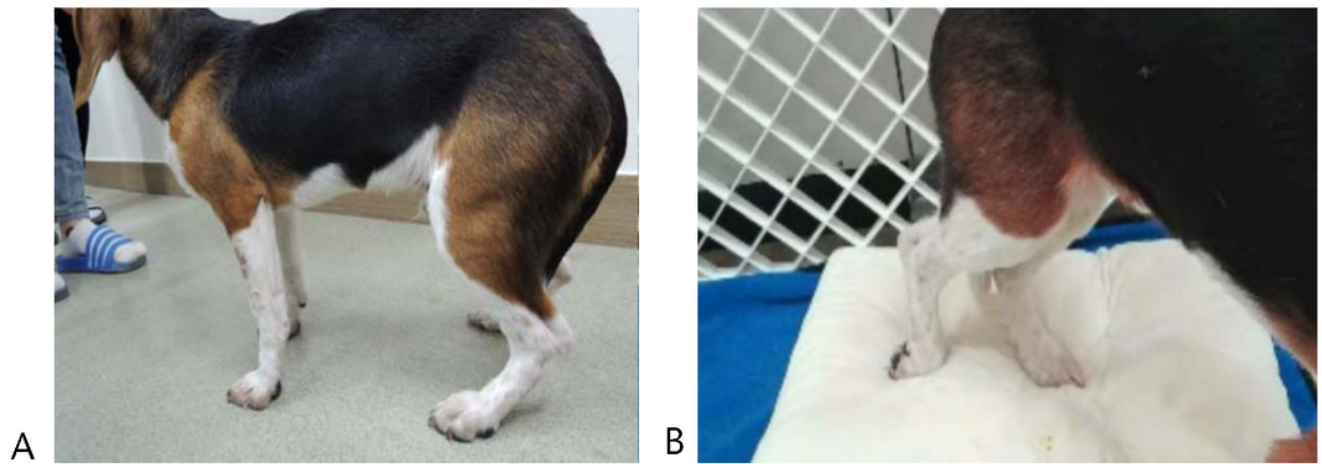


Figure 4

Behavior of 8-month-old cloned dog. **(A)** Flexed posture and **(b)** Knuckling test of transgenic dog

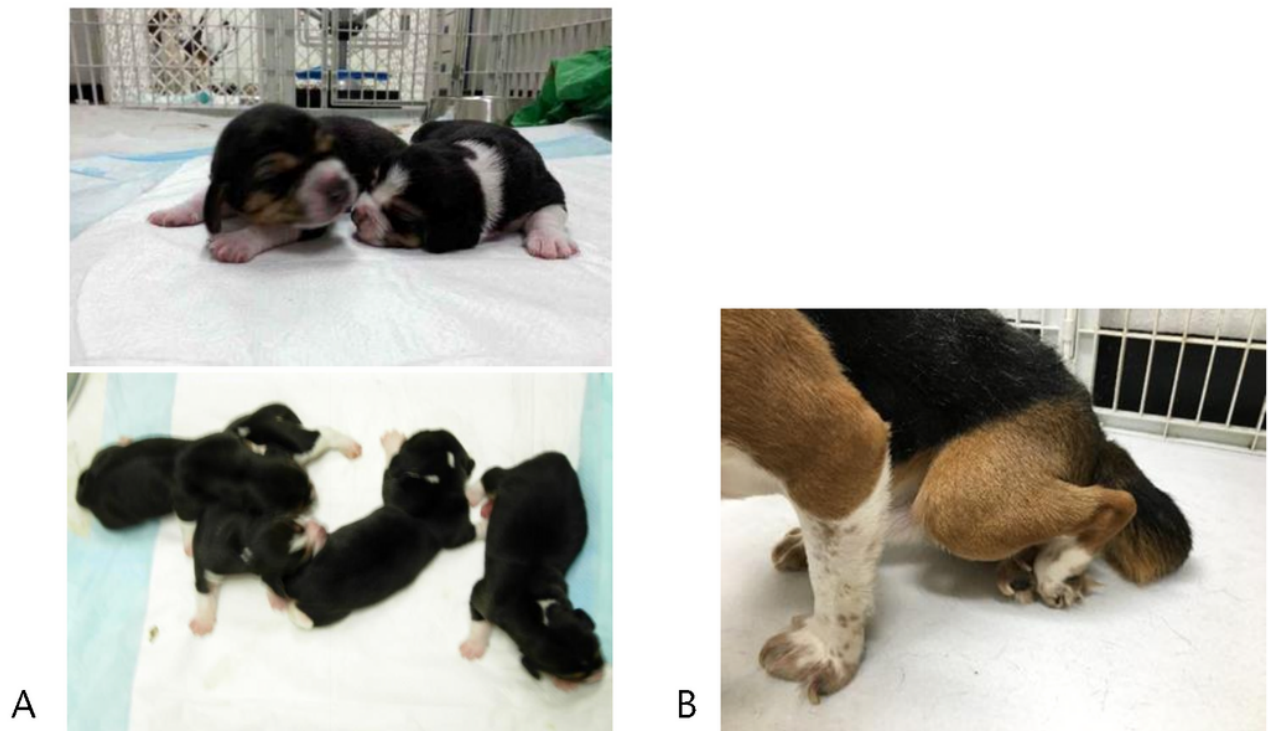


Figure 5

Offspring generated by artificial insemination using sperm samples of human protein deglycase DJ-1 gene (*hDJ-1*)-overexpressing transgenic dog. **(A)** Seven offspring of *hDJ-1* transgenic dog. **(B)** The 3-y-old dog who cannot straighten his toes.

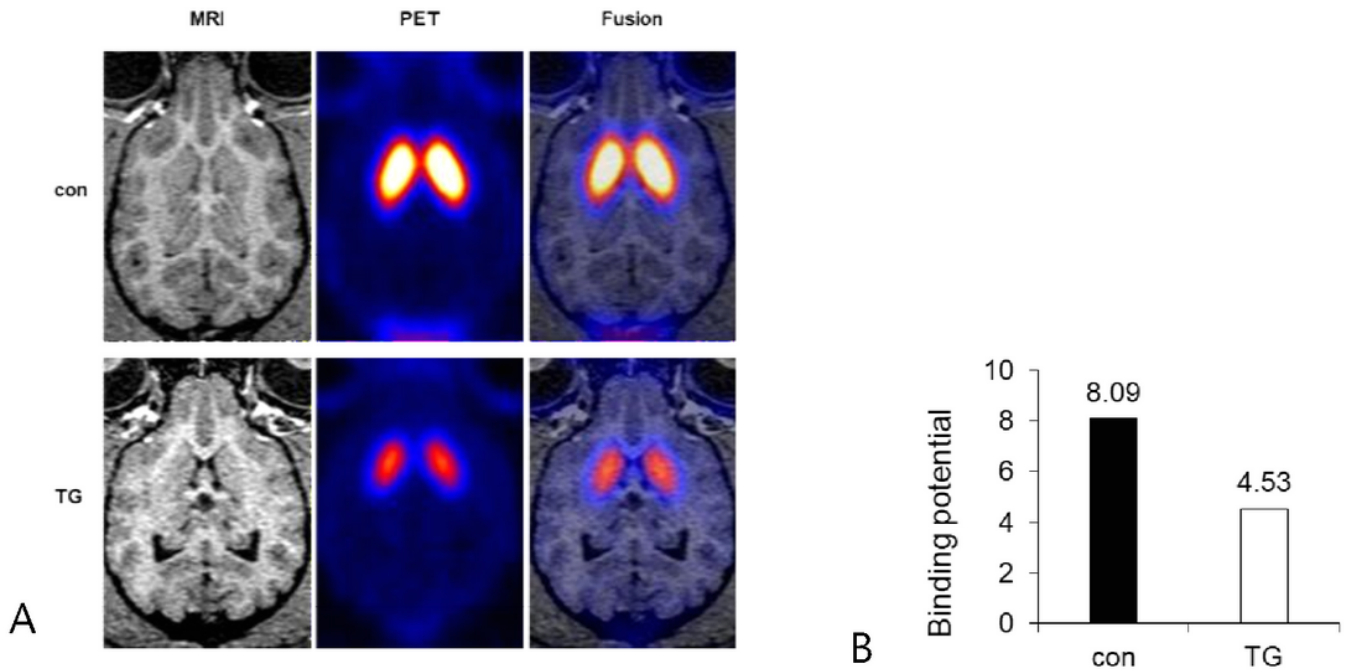


Figure 6

Positron emission tomography (PET) and magnetic resonance imaging (MRI) scans of 3-y-old human protein deglycase DJ-1 gene (*hDJ-1*)-overexpressing transgenic dog. **(A)** PET/MRI fusion images for N-(3- $[^{18}\text{F}]$ fluoropropyl)-2 β -carboxymethoxy-3 β -(4-iodophenyl) nortropane ($[^{18}\text{F}]$ -FP-CIT) uptake at the level of striatum. **(B)** $[^{18}\text{F}]$ -FP-CIT binding potential (BP) values in the striatum; BP values are means of both striata normalized by the cerebellum. Con, control dog; TG, *hDJ-1* transgenic dog

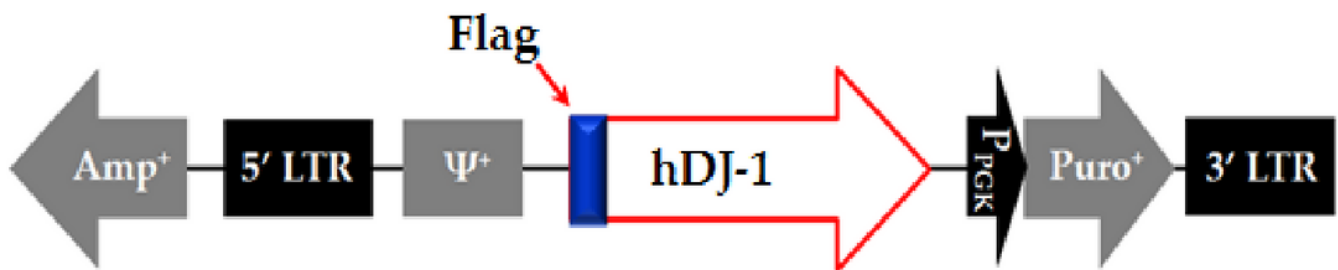


Figure 7

Construction of retroviral vector including human protein deglycase DJ-1 gene (*hDJ-1*). This vector contains the murine stem cell virus (MSCV) promoter, long terminal repeat (LTR), virus packaging signal (Ψ^+), puromycin resistance gene, and *hDJ-1* gene.

Supplementary Files

This is a list of supplementary files associated with this preprint. Click to download.

- [scirepsupplementaryfile.docx](#)
- [supplementaryvideos1.wmv](#)
- [supplementaryvideos2.wmv](#)
- [supplementaryvideos3.wmv](#)
- [supplementaryvideos4.wmv](#)